THE ARCHIVE OF MECHANICAL ENGINEERING

VOL. LV 2008 Number 4

DOI: 10.24425/ame.2008.131631

Key words: shell, constrained torsion, open cross section, buckling, experiments, finite elements

TOMASZ KOPECKI *

COUPLING EXPERIMENT AND NUMERICAL ANALYSIS IN THE STUDY OF POST-BUCKLING RESPONSE OF THIN-WALLED STRUCTURES

The paper presents the methodology that makes it possible to evaluate computational model and introduce current corrections to it. The methodology ensures proper interpretation of nonlinear results of numerical analyses of thin-walled structures.

The suggested methodology is based on carrying out, in parallel to nonlinear numerical analysis, experimental research on some selected crucial zones of load-carrying structures. Attention is drawn to the determinants concerning the performance of an adequate experiment. The author points out on indicating the role of model tests as a fast and economically justified research instruments practicable when designing thin-walled load-carrying structures.

The presented considerations are illustrated by an example of a structure whose geometrical complexity and ranges of deformation are characteristic for modern solutions applied in the load-carrying structures of airframes. As the representative example, one selected the area of the load-carrying structure that contains an extensive cut-out, in which the highest levels and stress gradients occur in the conditions of torsion evoking the post-buckling states within the permissible loads. The stress distributions within these ranges of deformations were used as the basis for determining the fatigue life of the structure.

1. Introduction

Rational approach to design of load-carrying structures seems to suggest the necessity of focusing special attention on crucial areas of these structures, which are decisive for durability and reliability of the structure. The presence of such crucial areas in a designed solution, resulting usually from its practical functions, should be given careful consideration in view of opportunity to introduce appropriate changes in the design solutions possibly before costly and time-consuming workshop realization of a prototype.

* *Faculty of Mechanical Engineering and Aeronautics, Rzeszów University of Technology, ul. W. Pola 2, 35-959 Rzeszów, Poland; E-mail: tkopecki@prz.edu.pl*

The intent of the author is to draw attention to the gravity of the factor of integrating nonlinear numerical analysis with an experiment - in a broad sense of this word. Then, this paper presents a methodology that can be used for assessment and current improvement of numerical models thus ensuring correct interpretation of results obtained from nonlinear numerical analyses of a structure.

The proposed methodology is based on carrying out experimental examination of selected crucial elements of load-carrying structures parallel with their nonlinear numerical analysis. Special attention is paid to factors determining proper realization of adequate experiments with emphasis placed on the role which the model tests can play as a fast and economically justified research tool that can be used in the course of design work on thin-walled load-carrying structures.

The presented considerations are illustrated by an example structure, whose degree of complexity and deformation range is characteristic for modern solutions in the design of airframe load-carrying structures. As a representative part of the construction design, we selected a fragment of a load-carrying structure containing an extensive cutout, in which the highest stress levels and gradients occur in the conditions of torsion resulting in post-buckling deformation states within the range of permissible loads, was selected. Stress distributions observed within that range of deformation constitute a basis for determination of the structure's fatigue life.

2. Subject and scope of research

The subject of the research was a thin-walled open-section cylindrical shell stiffened by means of longitudinal stringers (Fig. 1b), which model a zone with an extensive cutout (e.g. cockpit in an airframe structure). Such zones are usually joined with neighboring closed-section structural elements of cylindrical or slightly convergent shape. The planes of the joints determine boundary conditions eliminating the possibility of free deplanation of the outward sections.

A dimensioning form of load applied to the structure that, in the range of permissible load levels, can lead to loss of local stability of the shell, is the torsion retaining the character of a constrained one because of boundary conditions.

In order to determine the effect of longitudinal stiffening members on torsional rigidity within the full range of the analyzed deformations, structures with three, five and seven stringers were examined.

In the course of experimental work, photographic registration of subsequent deformation phases was carried out with simultaneous recording of vales of the torsion angle as the parameter enabling development of a representative

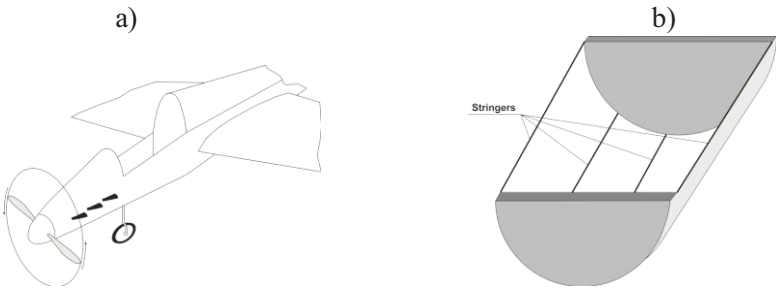

Fig. 1. (a) An example of extensive cutout in the airframe structure; (b) isolated, critical fragment of the structure

equilibrium path. The tests were carried out both in sub-buckling range and in advanced post-buckling deformation states.

In order to determine the stress field in post-buckling deformation states that could constitute a basis for numerical analysis of the structure's fatigue life, we developed a numerical model based on the finite elements method, for one of design solutions, was developed. The final shape of the model was developed on the grounds of comparative analysis of deformation patterns and the nature of representative equilibrium paths that were obtained experimentally and numerically.

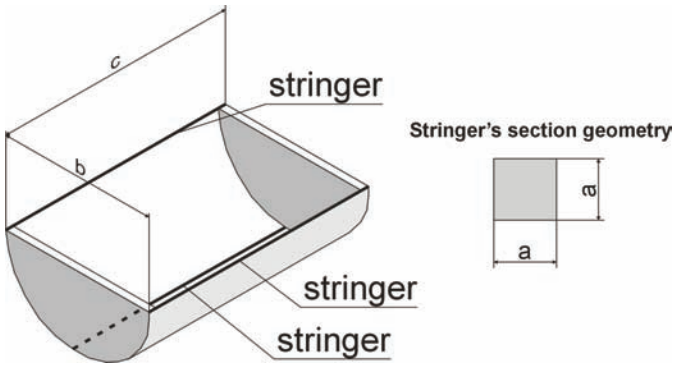

Fig. 2. Schematic geometry of the structure

3. Experimental research

Three variants of the examined structure, differed by the number of stringers were used. In the first variant, the structure was reinforced with three stringers, in the second one – with five, and in the third variant – with seven stringers. To reproduce boundary conditions ensuring torsional rigidity of the structure corresponding to the constrained torsion, both end sections of the shell were provided with 20 mm plates. Schematic diagram of the experimental setup is shown in Fig. 3.

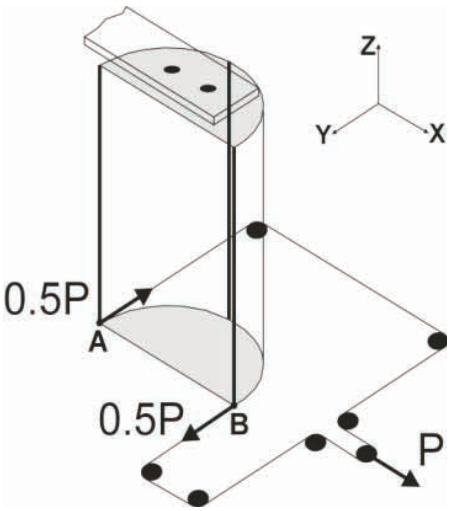

Fig. 3. Schematic diagram of the experimental setup

The structure was made of polycarbonate, for which the tensile strength test was carried out and material constants determined, i.e. Young's modulus E = 3000 MPa and Poisson ratio ν = 0.36.

Fig. 4 shows the characteristic of the above-mentioned material corresponding to one-dimensional tensile stress. Clearly visible elastic and inelastic deformation zones suggest the possibility that the actual material characteristic can be approximated by an ideal elastic-plastic model. Moreover, because of low value of its elasticity modulus (by two orders of magnitude lower than that of steel) it was possible to carry out experiments at low values of external loads.

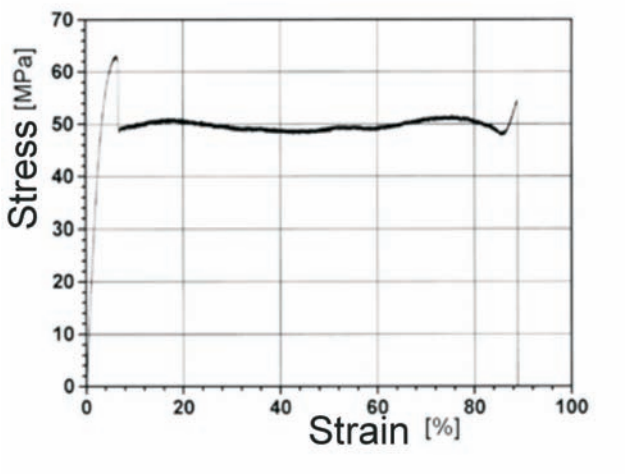

Fig. 4. Tensile stress plot for polycarbonate sample

The choice of the material, apart from the above-mentioned physical characteristics, was also justified by its high optical activity thanks to which it became possible to obtain qualitative information about optical effect distribution in circular polarization conditions. The Joints joints between the shell and the stringers were realized by means of steel bolts spaced 20 mm apart. In order to avoid possible assembly stress at bolt joints, continuous observation of isochromatic fringe pattern fields in the vicinity of each bolt was performed throughout the whole assembly work. A view of the experimental stand with the model mounted on it is presented in Fig. 5a.

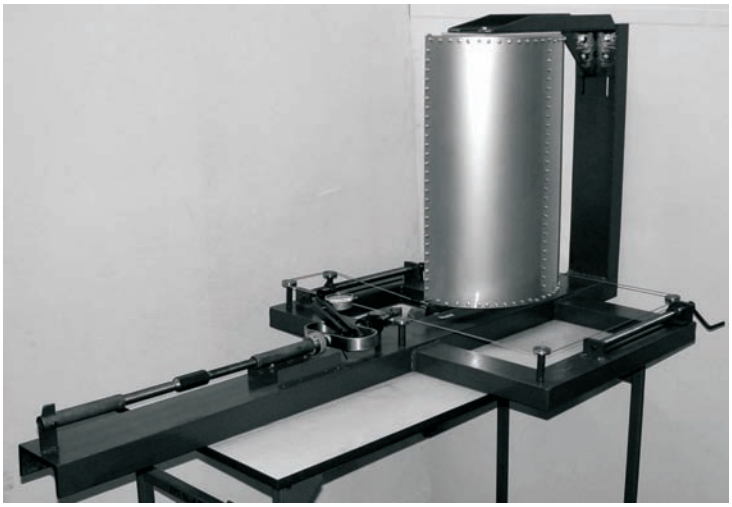

Fig. 5a. Experimental setup with the model fixed and ready for tests

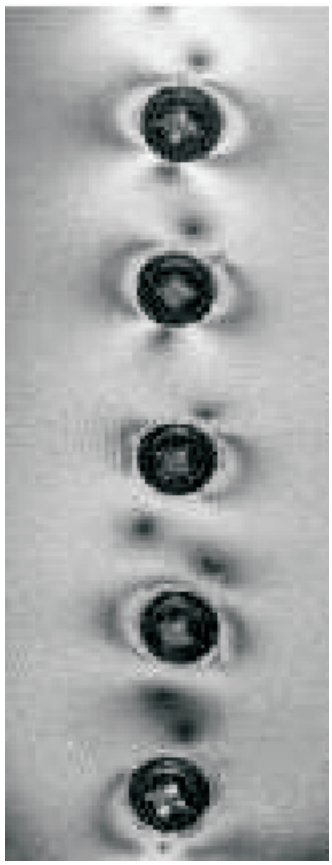

Fig. 5b. Distribution of isochromatic fringe patterns in vicinity of bolts subject to control during assembly

4. Structure reinforced with three stringers

The experimental work started with the structure reinforced by means of three stringers. The experiment was carried out with the load controlled by means of gravitational method ensuring good stability of load values. At the same time, one performed measurements of maximum values of the torsion angle. Based on these results, one determined a functional relationship between the twisting moment values and the model torsion angles representing an equilibrium path for a selected representative degree of freedom (cf. Fig. 6).

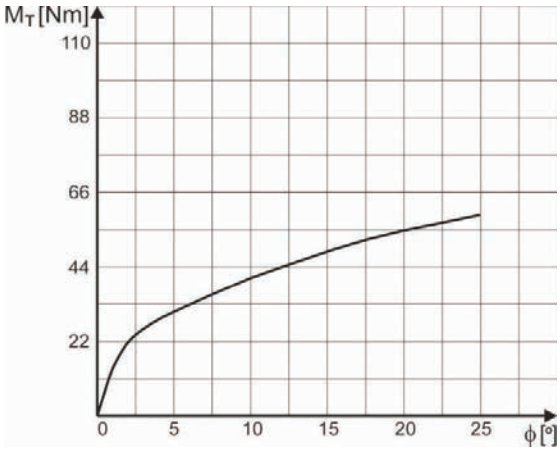

Fig. 6. Representative equilibrium path – a model with three stringers

The first perceptible indications of loss of stability were observed in the vicinity of frames and external stringers, at the twisting moment value of $M_t \approx 20$ Nm, corresponding to a torsion angle of $\Theta \approx 2^\circ$ (Fig. 6). While the load was increasing, the post-buckling equilibrium pattern covered larger and larger portion of the shell gradually reaching a global character.
Figures 7 and 8 present the initial phase of the loss of stability of the shell corresponding to the moment values of $M_t = 25$ Nm and $M_t = 35$ Nm, respectively.

It must be emphasized that the bifurcation-free character of the equilibrium path determined in the experiment was the result of the way in which the model was loaded and the possibility to perform the measurements only in steady-state conditions. Actually, the occurrence of large shell deformations and changes in their forms are connected with the jumps, in the course of which deformation increases although the load does not change. In fact, one deals here with a number of bifurcation processes, while the obtained equilibrium path represents the general character of dependence of the total torsion angle vs. twisting moment.

Fig. 9 presents an advanced form of post-buckling elastic deformation of the structure. The outward stringers were subject to significant deflection, while the central stringer did not change its original form. The obtained deformations confirm low torsional rigidity of the structure in advanced states, therefore it can be concluded that the use of solutions based on small number of stringers would be of little practical interest.

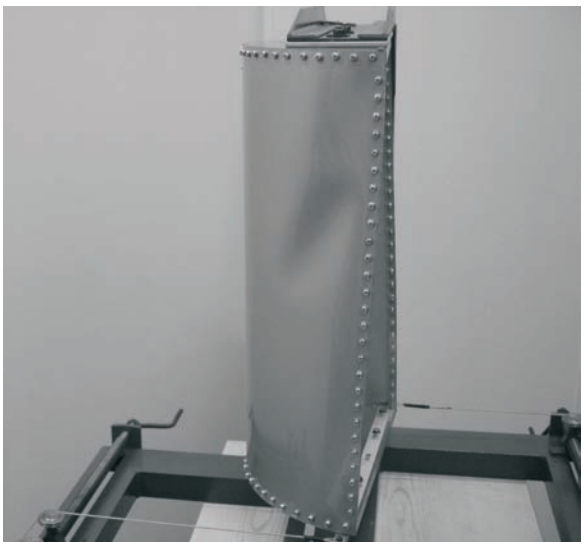

Fig. 7. Beginning of local buckling, M_t = 25 Nm

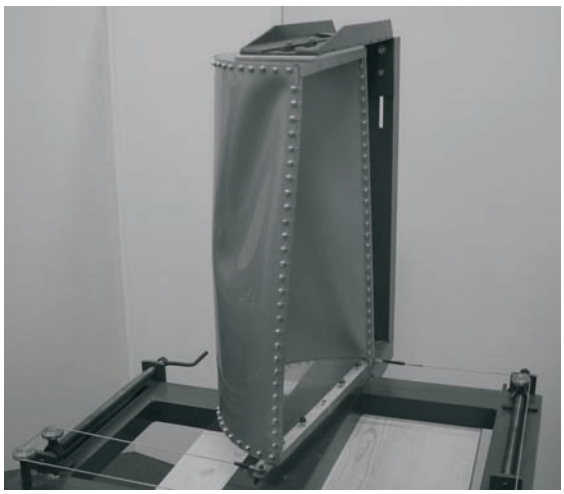

Fig. 8. Subsequent post-buckling deformation phase, M_t = 35 Nm

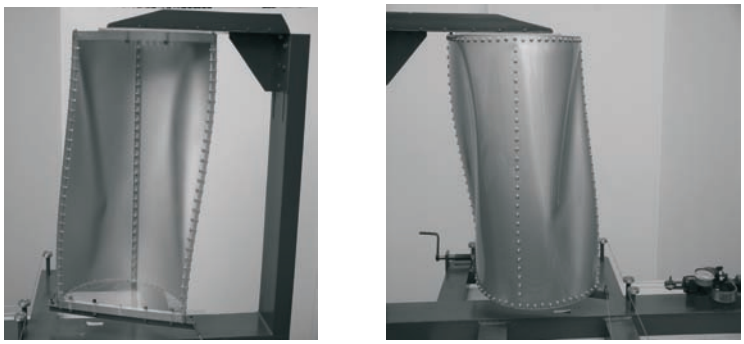

Fig. 9. Advanced post-buckling deformation, M_t = 60 Nm. M_t=60 Nm. (structure with three stringers)
View from the inside. View from the outside

5. Structure reinforced with five stringers

Another variant subject to examination represented a shell reinforced by means of five equally-separated stringers. The increase of the number of stringers was aimed at examining the expected increase of torsional rigidity, especially in advanced deformation states. As in the previous variant, the result of the experiment consisted in developing a plot showing the relationship between the twisting moment and the structure's torsion angle (Fig. 10).

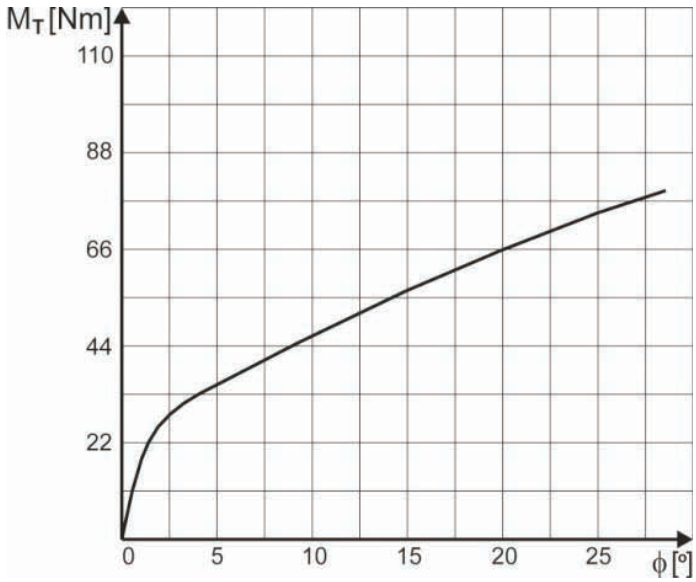

Fig. 10. Representative equilibrium path – a model with 5 stringers

The representative equilibrium path (Fig. 10) shows that loss of stability occurred here in a way similar to that observed in the case of structure

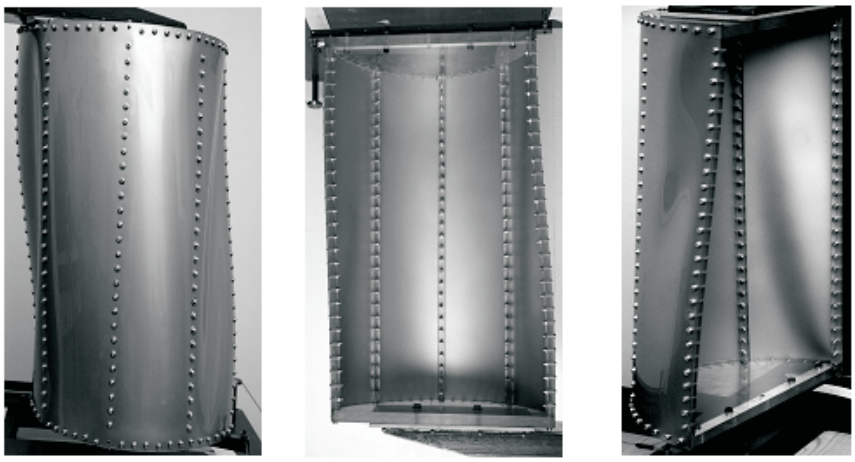

Fig. 11. Initial phase of post-buckling deformation (structure with 5 stringers), M_t = 35 Nm

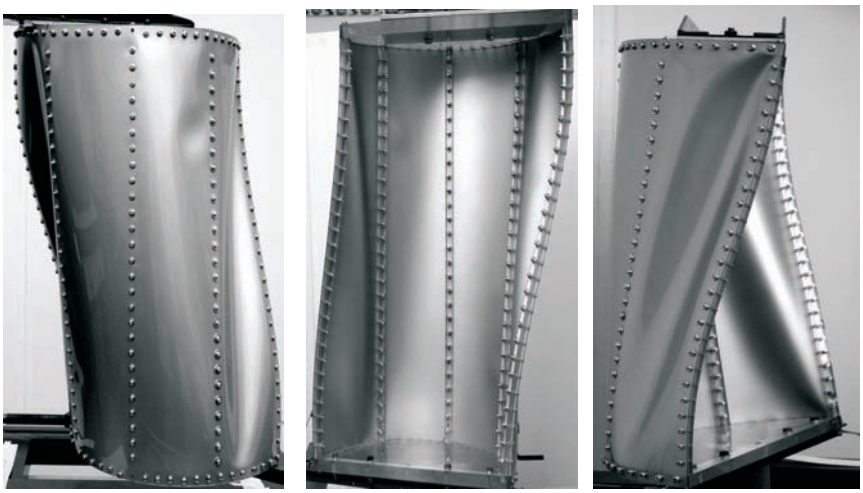

Fig. 12. Advanced post-buckling deformation phase (structure with 5 stringers), M_t = 75 Nm

with three stringers. The presence of additional stringers placed between the outward ones and the central member (Figs. 11 and 12) did not have any significant effect on rigidity of the examined structure.

6. Structure reiforced with seven stringers

The increase of the number of stringers to seven resulted in a significant increase of torsional rigidity of the structure. A considerable change was observed in the form in which the shell was loosing its stability, which consistinged in a distinct increase of load on the stringers. The relationship of the structure's torsion angle vs. the twisting moment obtained in the course of experiment is shown in Fig. 13. Post-buckling deformation patterns are

presented in Figs. 14 and 15. The process of local buckling was initiated in the vincinity of boundary stringers at twisting moment value of M_t = 33 Nm. Deformation of the shell proceeded smoothly. The experiment ended after the twisting moment reached M_t = 110 Nm. It was found that the largest deformations occurred in two outermost segments adjacent to the shell edges. The presence of additional stringers resulted in a decrease of the depth of the folds which, in fact, ment an increase of the system's torsional rigidity. Deformations of the shell and stringers in the central part of the structure remained small compared to the deformations observed in the first two variants.

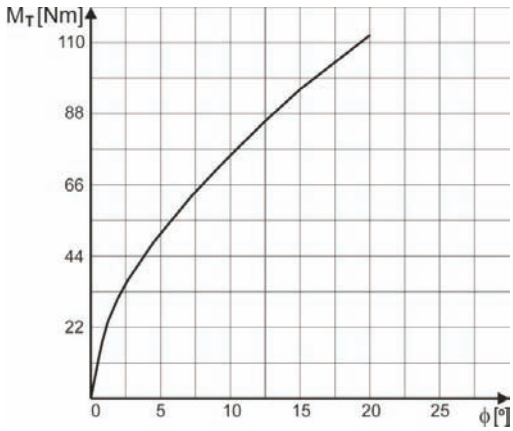

Fig. 13. Equilibrium path – a model with 7 stringers

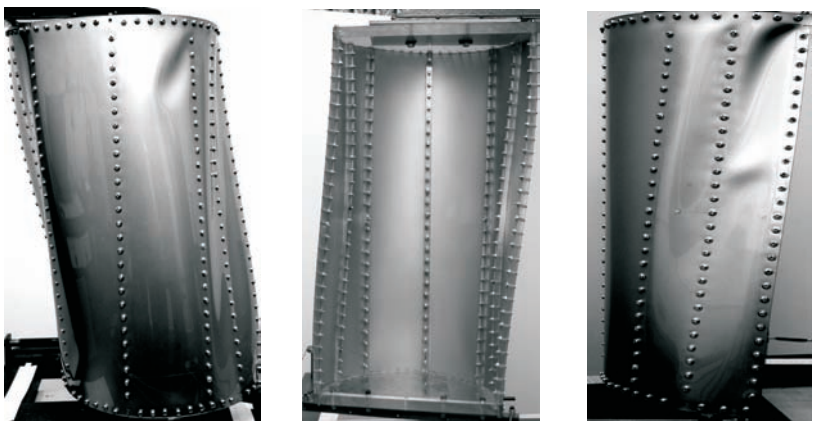

Fig. 14. Initial phase of deformation (structure with 7 stringers). M_t=55 Nm

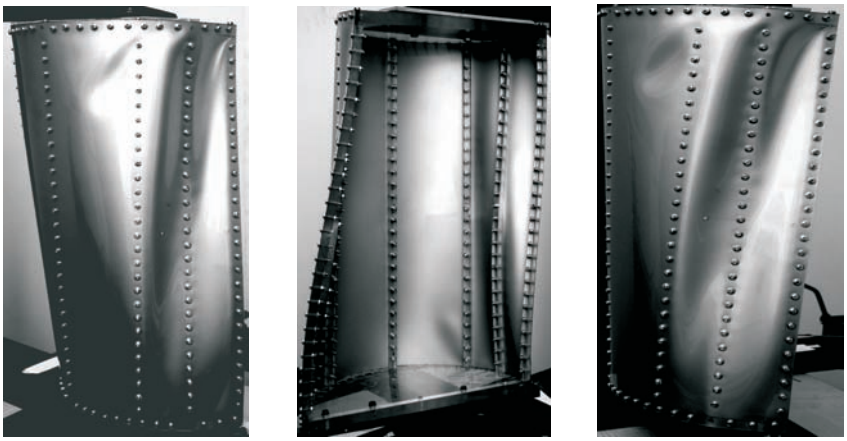

Fig. 15. Advanced post-buckling deformation pattern (structure with 7 stringers). M_t=110 Nm

Fig. 16 presents a comparison of three characteristics corresponding to the three analyzed solutions of the structure design. In comparison with the first two variants, the structure reinforced with seven stringers revealed a significant increase of torsional rigidity. For instance, at twisting moment value M_t = 55 Nm, the torsion angle of the structure with three stringers amounted to 20° compared to only about 6° in the case of the third variant. The applied reinforcement shows therefore a significant effect on the increase of torsional rigidity as well as on the values and patterns of stress distribution in the structure.

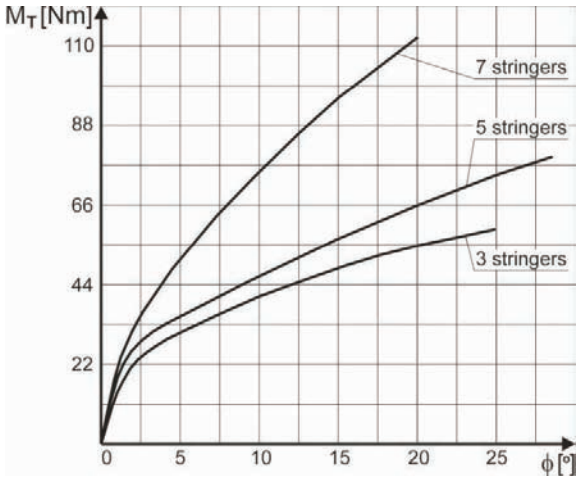

Fig. 16. Comparison of representative equilibrium paths

7. Examination by means of optical polarization methods

Optical sensivity of the material of which the test structure was constructed allowed for observation of distributions of optical effects in polarized light. In the case of bending/membrane state occurring in post-buckling deformation conditions, the optical effect observed in circularly-polarized light can not be identified with isochromatic fringe patterns as the principal stress axes can vary along the shell thickness. These effects are overestimated compared to isochromatic fringe pattern values, and the degree of overestimation increases with the increasing angle between the directions of principal stressesof bending and membrane states [10, 11,12]. The quantitative analyses of the observed patterns can be biased with a significant error. Nevertheless, the observed optical effects represent a source of vital information useful in determination of high stress gradients zones, and this information that can then be particularly helpful when developing a numerical model aimed at determination of stress fields characteristic for advanced post-buckling deformation states.

Figs. 17-20 present an example distributions of optical effects observed in the examined models are.

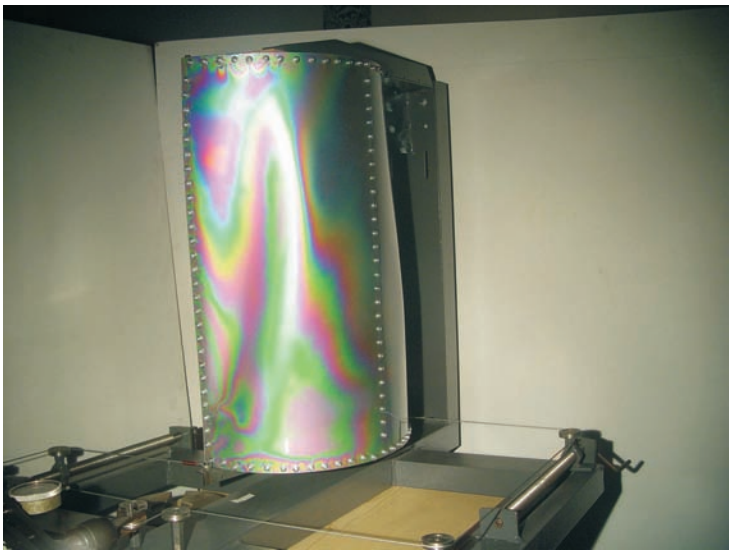

Fig. 17. Optical effect distributions. A model with 3 stringers

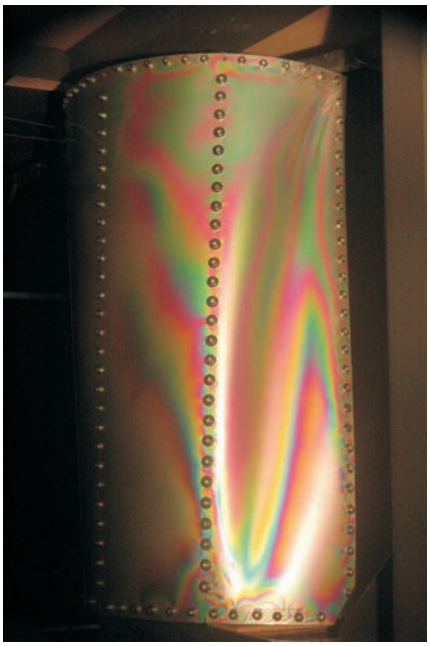

Fig. 18. Optical effect distributions. A model with 5 stringers

Fig. 19. Optical effect distributions – a model with 5 stringers

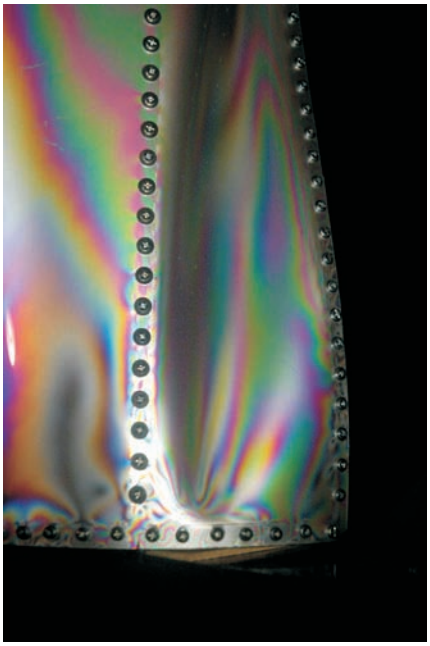

Fig. 20. Optical effect distributions – a model with 5 stringers

8. Numerical analysis

In the non-linear numerical analysis of load-carrying structures, relations between the set of static and of suitable them geometric parameters can be presented in the form of matrix equation:

$$\mathbf{g} = \mathbf{K}^{-1}(\mathbf{g})\,\mathbf{f}, \tag{1}$$

where **g** is the set of geometric parameters describing the state of deformation of the structure that triggers off loading, **f** constitutes the set of static parameters and **K** is the stiffness matrix dependent on the set of geometric parameters determining the current state of deformation of the non-linear constitutive relation and other factors.

In the considered issue, plastic strains were not observed in the whole range of deformations during experimental studies (also after unloading). And so, a linear constitutive relation was accepted, keeping the assumption about invariance of the normal interval ($\varepsilon_{\mathbf{z}} = \mathbf{0}$):

$$\sigma = \mathbf{D}\varepsilon \tag{2}$$

where $\boldsymbol{\sigma} = \left\{\boldsymbol{\sigma}_{\mathbf{x}}, \boldsymbol{\sigma}_{\mathbf{y}}, \boldsymbol{\tau}_{\mathbf{xy}}, \boldsymbol{\tau}_{\mathbf{yz}}, \boldsymbol{\tau}_{\mathbf{zx}}\right\}^{T}$ is a vector of the stress state components,

$$\mathbf{D} = \frac{E}{1-\nu^2}\begin{bmatrix} 1 & \nu & 0 & 0 & 0 \\ \nu & 1 & 0 & 0 & 0 \\ 0 & 0 & \dfrac{1-\nu}{2} & 0 & 0 \\ 0 & 0 & 0 & \dfrac{1-\nu}{2k} & 0 \\ 0 & 0 & 0 & 0 & \dfrac{1-\nu}{2k} \end{bmatrix} \tag{3}$$

is the matrix of material constants, in which, one take into account the influence of shear strains on elastic energy of the shell using the corrective ratio **k=1.2**, [16],

$$\boldsymbol{\varepsilon}=\left\{\varepsilon_x, \varepsilon_y \gamma_{xy}, \gamma_{yz}, \gamma_{zx}\right\}^T=\left\{\begin{array}{c} \dfrac{\partial u}{\partial x}+\dfrac{1}{2}\left[\left(\dfrac{\partial u}{\partial x}\right)^2+\left(\dfrac{\partial v}{\partial x}\right)^2+\left(\dfrac{\partial w}{\partial x}\right)^2\right] \\ \dfrac{\partial v}{\partial y}+\dfrac{1}{2}\left[\left(\dfrac{\partial u}{\partial y}\right)^2+\left(\dfrac{\partial v}{\partial y}\right)^2+\left(\dfrac{\partial w}{\partial y}\right)^2\right] \\ \dfrac{\partial u}{\partial y}+\dfrac{\partial v}{\partial x}+\left(\dfrac{\partial u}{\partial x}\right)\left(\dfrac{\partial u}{\partial y}\right)+\left(\dfrac{\partial v}{\partial x}\right)\left(\dfrac{\partial v}{\partial y}\right)+\left(\dfrac{\partial w}{\partial x}\right)\left(\dfrac{\partial w}{\partial y}\right) \\ \dfrac{\partial u}{\partial z}+\dfrac{\partial w}{\partial y}+\left(\dfrac{\partial u}{\partial y}\right)\left(\dfrac{\partial u}{\partial z}\right)+\left(\dfrac{\partial v}{\partial y}\right)\left(\dfrac{\partial v}{\partial z}\right)+\left(\dfrac{\partial w}{\partial y}\right)\left(\dfrac{\partial w}{\partial z}\right) \\ \dfrac{\partial u}{\partial z}+\dfrac{\partial w}{\partial x}+\left(\dfrac{\partial u}{\partial x}\right)\left(\dfrac{\partial u}{\partial z}\right)+\left(\dfrac{\partial v}{\partial x}\right)\left(\dfrac{\partial v}{\partial z}\right)+\left(\dfrac{\partial w}{\partial x}\right)\left(\dfrac{\partial w}{\partial z}\right) \end{array}\right\} \tag{4}$$

is a vector of strain state components corresponding to the Green – Saint-Venant tensor, and ***u, v, w*** are displacement components in the local coordinate system ***x, y, z***.

Numerical representation of nonlinear deformation of load-carrying structures are based on the assumption that, at any stage of the solution, the deformed system remains in the state of static balance. And so, for the defined discrete system, it is possible to formulate the set of the equilibrium equations, which, when applied to the nonlinear structural analysis, formulated in the displacement method, can be presented in the form of the matrix equation of residual forces [5]:

$$\mathbf{r}(\mathbf{u}, \boldsymbol{\Lambda}) = \mathbf{0}, \tag{5}$$

where **u** is the state vector, containing displacement components of the structure nodes, which corresponds to the current geometric configuration, Λ is the matrix containing control parameters corresponding to the current level of the loading, and **r** is a residual vector containing unbalanced components

of the forces, corresponding to the current state of the structure deformation [4,5]. The **r** vector represents the gradient of the total potential energy of the system – $\approx \mathbf{\Pi}(\mathbf{u}, \mathbf{\Lambda})$:

$$\mathbf{r} = \frac{\partial \mathbf{\Pi}}{\partial \mathbf{u}}. \tag{6}$$

It means that a zero increase of the potential energy is the condition for the static equilibrium of the considered structure. The stiffness matrix **K(g)**, corresponding to the current geometry configuration, is the derivative of vector **r** with respect to the components of the state vector **u**:

$$\mathbf{K} = \frac{\partial \mathbf{r}}{\partial \mathbf{u}}. \tag{7}$$

The components of the $\mathbf{\Lambda}$ matrix are expressed in the function of the $\boldsymbol{\lambda}$ parameter determined as the control parameter of the state. This parameter is a measure of the increment of the loading, connected indirectly or directly with a pseudo-time parameter – **t**. And so, the set of the equilibrium equations (5) can be presented in the form:

$$\mathbf{r}(\mathbf{u}, \lambda) = \mathbf{0}, \tag{8}$$

The above equation is determined as a single-parametric equation of residual forces. Its solution presents the determined number of the subsequent states of structure deformation. For every state, there is a combination of changing control parameters, connected with loading of the structure, expressed by the single control parameter – λ.

The process of the incremental step transition, from the current state to the next one, is initiated by the change of the control parameter, which corresponds to the new structure geometry, determined by the new state vector. The turn from the current state to the next, presenting incremental step, is initiated by the change of the control parameter, which the new geometrical configuration of the structure, described by a new state vector, corresponds to.

The development of numerical methods, reflected that were applied in the contemporary algorithms, included in professional, commercial software, establish resulted in two basic kinds of methods of determining the subsequent equilibrium states. The first, and the basic group, are purely incremental methods, the so-called prognostic method. The second group are the corrective methods, called the prediction-correction or prediction-iteration methods. The methods belonging to the first group are characterized by a limited, often unsatisfactory accuracy of the results they yield. A corrective phase is introduced mainly in order to reduce the solution error and to allow to determining the critical points on the equilibrium path. It provides the possibility

of analysis of the structure in advanced deformation states. The common feature of both kinds of methods, is the presence of the incremental phase. The essence of the solution procedure of non-linear problem is that during the transition from the **n** state to next – **n+1**, the undetermined quantities are:

$$\Delta \mathbf{u_n} = \mathbf{u_{n+1}} - \mathbf{u_n} \text{ and } \Delta \boldsymbol{\lambda}_\mathbf{n} = \boldsymbol{\lambda}_{\mathbf{n+1}} - \boldsymbol{\lambda}_\mathbf{n} \ . \tag{9}$$

In order to determine that these quantities, it is necessary to formulate additionally equation, called equation of incremental control or equation of constraint equation:

$$\mathbf{c}(\Delta \mathbf{u_n}, \Delta \boldsymbol{\lambda}_\mathbf{n}) = \mathbf{0}, \tag{10}$$

The basic component of the incremental phase constitutes the prognostic step. It determines the point in the state hyperspace, corresponding to the subsequent geometrical configuration of the system, determined by defining the increment $\Delta\mathbf{u}$ for the assumed $\Delta\boldsymbol{\lambda}$, under the assumption that equation (10) is satisfied. The error of the solution in the particular incremental step depends on the constraint equation. The important thing is that in every subsequent incremental step, the value of total error can increase, which is determined as the drift error. The corrective phase ensures that this error is minimized.

The basic method of the solution of non-linear problems is the Newton – Raphson method [2,14,16]. There is a number of variants, which constitute the so-called family of the Newton-like methods. The essence of these methods consists in expanding the equations of residual forces **r=0** and incremental control **c=0** into Taylor series.
Assuming that in the "k-th" step of the iteration one obtains the values $\mathbf{u}^\mathbf{k}$ and $\boldsymbol{\lambda}^\mathbf{k}$, the mentioned equations can be presented in the form:

$$\mathbf{r}^{k+1} = \mathbf{r}^k + \frac{\partial \mathbf{r}}{\partial \mathbf{u}} \cdot \mathbf{d} + \frac{\partial \mathbf{r}}{\partial \lambda} \cdot \eta + \boldsymbol{W.R.} = \mathbf{0}, \tag{11}$$

$$c^{k+1} = c^k + \frac{\partial c}{\partial \mathbf{u}} \cdot \mathbf{d} + \frac{\partial c}{\partial \lambda} \cdot \eta + \boldsymbol{W.R.} = \mathbf{0}, \tag{12}$$

where

$$\mathbf{d} = \mathbf{u}^{\mathbf{k+1}} - \mathbf{u}^\mathbf{k}, \quad \boldsymbol{\eta} = \boldsymbol{\lambda}^{\mathbf{k+1}} - \boldsymbol{\lambda}^\mathbf{k} \tag{13}$$

The terms ***W.R.*** located in both equations represent negligible residual values of higher orders. In the following iterative process, the consecutive values of **d** and η are determined, in reference to which one checks the

condition of convergence for the assumed tolerance. The set of solutions, obtained by solving the nonlinear system of algebraic equations with respect to unknown nodal displacements for the determined range of loading, gives the base to create an equilibrium path. This path, as the relationship between the static parameters corresponding to the load of the structure and the geometric parameters associated with displacements of the nodes, constitutes a hyper-surface in a multidimensional space, where number of dimensions corresponds to the number of degrees of freedom of the system. In practice, in order to present the equilibrium path in a two-dimensional coordinate system, one creates the relations between the control parameter and the representative state parameter are.

In the considered issue, one accepted the maximum values of torsion angle of the structure and the twisting moment of a couple of the forces, acting on the frame closing the boundary section as representative parameters for determining the equilibrium path. As a base of the analysis process, one applied the Newton – Raphson method and the corrective strategy based on arc-length control concept formulated by Riks – Wempner [11,16]. The attempts to apply the Newton – Raphson method without the correction phase, did not allow for obtaining a convergent solution. Reliability of the obtained results was assessed by comparing the equilibrium path to the result of experiment, as well as assessing the compatibility of deformations obtained in the numerical way and those obtained experimentally. Information from both of these comparisons suggesting the necessity of making multiple corrections in the numerical models. Creating those such models, one took into consideration a number of factors resulting from the necessity to retain some features of the real structure. Most important was to use a correct set of finite elements to make an appropriate simplifications in the geometry of the modeled structure and to appropriate reproduce the boundary conditions. In order to meet the above requirements, it was necessary to perform a number of numerical tests. Fig 21 illustrates the concept of boundary conditions reproduction, according to which the nodes fixing the structure are represented by two constraint points with blocked translational and rotational degrees of freedom. This corresponds to the real manner of fixing the structure by means of two bolts fastening one of the outward frames to the test stand.

Nonlinear numerical analyses were performed using the MSC MARC-2007 software package. Several model versions of the structure, with three stringers, and with various ways of reproduction of stringers and their joints with the shell were created.

In all cases, the shell was modeled using a curved, quadrilateral, thin-shell element. This is was an isoparametric, double-curved thin-shell element

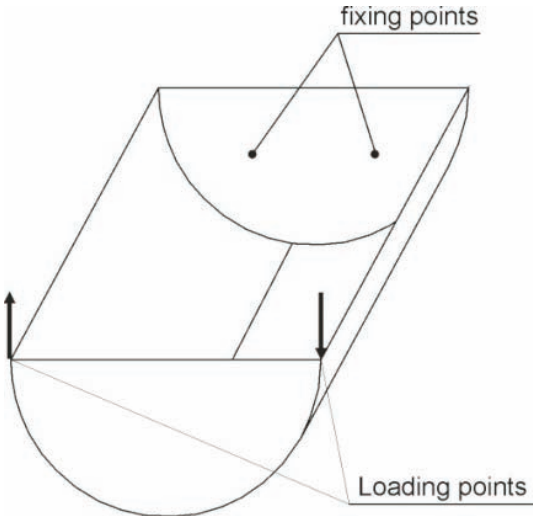

Fig. 21. Schematic diagram of model fix and load

using bicubic interpolation functions, based on Koiter-Sanders shell theory. There are the following 12 degrees of freedom at each node:

$$u, \frac{\partial u}{\partial \theta^1}, \frac{\partial u}{\partial \theta^2}, v, \frac{\partial v}{\partial \theta^1}, \frac{\partial v}{\partial \theta^2}, w, \frac{\partial w}{\partial \theta^1}, \frac{\partial w}{\partial \theta^2}, \frac{\partial^2 u}{\partial \theta^1 \partial \theta^2}, \frac{\partial^2 v}{\partial \theta^1 \partial \theta^2}, \frac{\partial^2 w}{\partial \theta^1 \partial \theta^2},$$

where (θ^1, θ^2) denote Gaussian coordinates on the middle surface of the shell. Large deformation analysis allows the Lagrangian description. Large deflection terms corresponding to the stretching strains were introduced. This approximation is acceptable for nonlinear buckling analysis.

The frames, and in some cases the stringers, were modeled using bilinear, four-node thick-shell element with global displacement and rotations as the degree of freedom. Bilinear interpolation was used for the coordinates, displacement and the rotations. The six degrees of freedom per node are as follows:

u, v, w – displacement components defined in global Cartesian x,y,z – coordinate system,

$\mathbf{\Phi_x}, \mathbf{\Phi_y}, \mathbf{\Phi_z}$ – rotation components about global: **x, y, z** – axis respectively.

In order to reproduce the structure stiffness ensuring compatibility with experiment results, three kinds of elements were applied for the modeling the stringers: bilinear thick-shell element, elastic beam element and three-dimensional arbitrary-distorted brick elements.

Elastic beam with transverse shear is a straight beam in space which includes transverse shear effects with elastic material response. Linear interpolation iwas used for the axial and the transverse displacements as well as for the

rotations. The output section forces are output aswere: the axial force, local, $\mathbf{T_x}$ $\mathbf{T_y}$ – shear forces, bending moments about the **x, y** – axes of the cross section respectively, torque moment about the beam axis.

The three-dimensional arbitrary-distorted brick element is an eight-node, isoparametric, arbitrary hexahedral. As this element uses trilinear interpolation functions, the strains tend to be constant throughout the element. The element can be used for all the constitutive relations. There are three global degrees of freedom: u, v, w – at each node. In the one of the models, joints between stringers and the shell were reproduced in a discrete way, by means of beam-type elements, with a simultaneous use of contact preventing elements interpenetrate in advanced deformation states. In other cases, joints of continuous kind were used. The results of calculation show that the way in which the joints between shell and stringers were modeled, had little influence on the character of effective stress distribution in the structure shell. Moreover, the model with discrete joints is characterized by high complexity, which – as it was proved in numerical tests - makes the convergence of nonlinear analyses much more difficult to obtain and leads to deformation patterns incompatible with those obtained in the experimental way in the post-buckling range.

Fig. 22 presents comparison of effective stress distribution according to Huber-Mises-Hencky criterion in the pre-buckling range, for the models with stringers constructed of 3D elements and joints realized by means of two different methods.

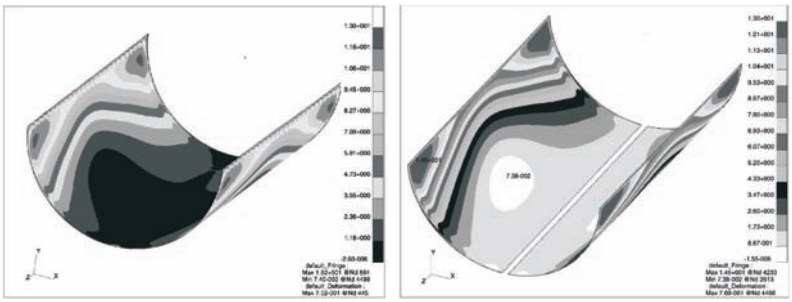

Fig. 22. Comparison of stress distributions in the middle layer according to HMH hypothesis obtained for the discrete joints model (left) and the continuous joints model (right)

Conformity of deformations was obtained for two version of the models, with continuous joints. In the first one, the stringers made of three-dimensional elements were used. In the second case, one applied one-dimensional stringers, made of beam-type elements. Comparison of the calculated deformation patterns corresponding to maximum load with the deformation observed in the course of experimental investigation is presented in Fig. 23.

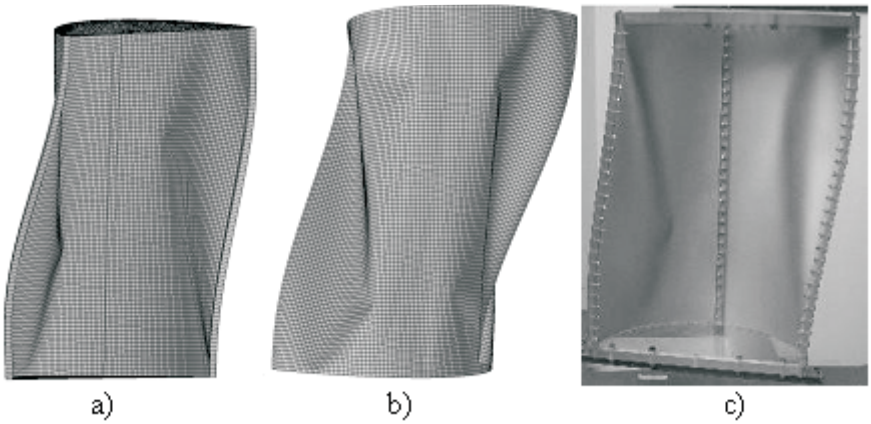

Fig. 23. Post-buckling deformation patterns under the same load: (a) a model with stringers made of 3D elements; (b) a model with stringers made of beam elements; (c) actual structure under load

For both models, the equilibrium paths representing the relationship of twisting moment vs. torsion angle, complied with the similar ones, measured experimentally. The comparison of equilibrium paths obtained by means of numerical calculations with the results of experiment is presented in Fig. 24.

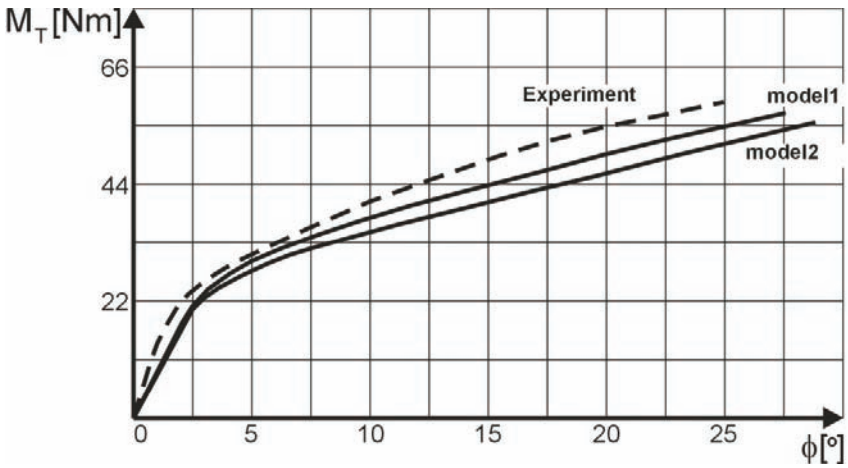

Fig. 24. Comparison of representative equilibrium paths: model1 – stringers of 3D elements; model2 – stringers of beam elements

By comparing the values of the representative state parameter (torsion angle) pertaining to specific values of the control parameter (twisting moment) one can conclude that the maximum divergence between results obtained numerically with those measured in the experiment for the highest applied loads amounts to about 30%. As it follows from the above comparison of the characteristics, the model reproducing stiffness of stringers based on 3D elements shows a better conformity with experiment than the model based

on beam elements. The obtained convergence of equilibrium paths and deformation patterns allows us to conclude that stress distributions obtained as the result of numerical analyses are close to the actual ones, and therefore can be adopted as a basis for estimates concerning durability of the structure. Fig. 25 presents comparison of stress distributions according to Huber-Mises-Hencky hypothesis for different deformation phases. The analysis of that juxtaposition leads to the conclusion that in the post-buckling deformations phase some significant redistribution of stresses occur, and therefore the use of simplified calculation algorithms based on linearized analysis of stability has no grounds in the case of structures of that type.

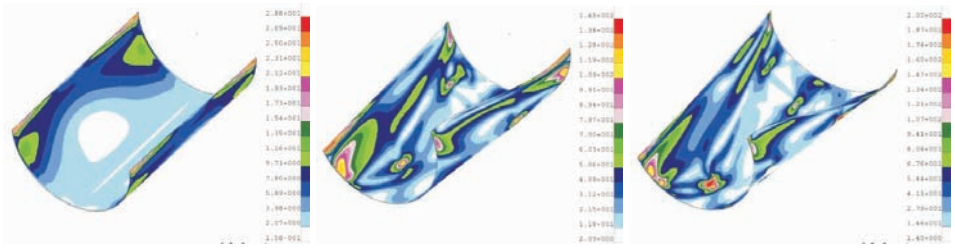

a) b) c)

a) 25% load — middle layer; b) 70% load — middle layer;
c) 100% load — middle layer

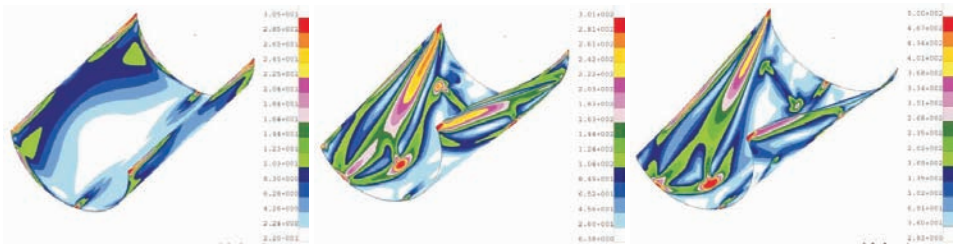

d) e) f)

Fig. 25. Stress distributions according to HMH hypothesis (a model with stringers represented by beam elements): d) 25% load – external layer; e) 70% load – external layer; f) 100% load – external layer

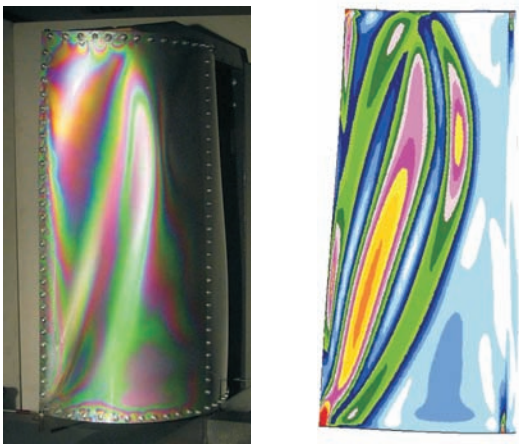

Fig. 26. Comparison of isochromatic fringe pattern distribution in the experimental model with stress distribution according to H-M-H hypothesis – a model with three stringers

9. Conclusions

The performed numerical analyses and experimental investigation lead to several conclusions of, how as it seems, cognitive and utilitarian significance. The concept of performing the numerical analyses associated with experiment refers to the observed tendency, according to which the contemporary design of load-carrying structures, should be supported by permanent improvement of numerical formulations. The common feature of the two approaches to structure design is idealization of structures. We have in mind that, in engineering applications, the FEM is an approximate method, and the received results refers not to the real structure, but to an idealized model. So that, without denying the importance of non-linear numerical analyses as tools of unquestionable effectiveness, we must keep in mind the problem of unreliability of results. It seems then that experimental verifications of FEM analyses is justified and sometimes indispensable. Such verification significantly increases reliability of results obtained on the numerical way.

Despite the limitations connected with the possibilities of proper interpretation of optical effects, analyzed in terms of quality considerations, the results of photo-elastic examinations may provide the significant information about the existence of stress concentration areas in pre-buckling and post-buckling states, even before numerical models are created.

The results of experimental investigation used for improving numerical models and for correcting computing procedures, pointed at the necessity of taking into consideration the corrective phase of nonlinear analysis. Neglecting this phase leads to incompatibilities of numerical and experimental results or may resort in the lack of convergence of the solution.

It is necessary to emphasize that compatibility of deformations in experimental and numerical models validated the credibility of stress fields received as the result of numerical computation.

There are some other, more detailed remarks and conclusions that follow on the suggested procedure. For example, the results of numerical analyses and experimental examinations proved, that the method of modeling of connections between the stringers and the shell did not have any significant effect on the character of global deformation. It is also important to notice that the model based on stringers fixed with discrete connections to the shell, which has great complexity, makes it more difficult to obtain a convergent solution in the non-linear analysis.

Manuscript received by Editorial Board, April 24, 2008;
final version, November 19, 2008.

REFERENCES

[1] Arborcz J.: Post-buckling behavior of structures. Numerical techniques for more complicated structures. Lecture Notes In Physics, 228, 1985.
[2] Bathe K. J.: Finite element procedures. Prentice Hall, 1996.
[3] Doyle J. F.: Nonlinear analysis of thin-walled structures. Springer-Verlag, New York Berlin Heidelberg, 2001.
[4] Felippa C. A., Crivelli L. A., Haugen B.: A survey of the core-congruential formulation for nonlinear finite element. Archives of computational methods in engineering 1, 1994.
[5] Felippa C. A.: Procedures for computer analysis of large nonlinear structural system in large engineering systems. ed. by A. Wexler, Pergamon Press, London, 1976.
[6] Kopecki H.: Problemy analizy stanów naprężenia ustrojów nośnych, w świetle badań eksperymentalnych metodami mechaniki modelowej, Zeszyty Naukowe Politechniki Rzeszowskiej, Nr 78, Rzeszów, 1991.
[7] Królak M., Młotkowski A.: Experimental analysis of post-buckling and collapse behaviour of thin-walled box-section beam. Thin-Walled Structures, 26:287-314, 1996.
[8] Laerman K. H.: The principle of integrated photo-elasticity applied to experimental analysis of plates with nonlinear deformation. Proc. 7th Conf. on experimental stress analysis, Haifa, 1982.
[9] Lynch C.: A finite element study of the post buckling state behaviour of a typical aircraft fuselage panel. PhD. Thesis, Queen's University Belfast, 2000.
[10] Lynch C., Murphy A., Price M., Gibson A: The computational post buckling analysis of fuselage stiffened panels loaded in compression. Thin-Walled Structures, 42:1445-1464, 2004.
[11] Marcinowski J.: Nieliniowa stateczność powłok sprężystych. Oficyna Wydawnicza Politechniki Wrocławskiej, Wrocław 1999.
[12] Mohri F., Azrar L., Potier-Ferry M.: Lateral post buckling analysis of thin-walled open section beams. Thin-Walled Structures, 40:1013-1036, 2002.
[13] Niu M. C.: Airframe structural design. Conmilit Press Ltd., Hong Kong, 1988.
[14] Rakowski G., Kacprzyk Z.: Metoda elementów skończonych w mechanice konstrukcji. Oficyna Wydawnicza Politechniki Warszawskiej, Warszawa, 2005.
[15] Ramm E.: The Riks/Wempner Approach – An extension of the displacement control method in nonlinear analysis. Pineridge Press, Swensea, 1987.

[16] Zienkiewicz O. C., Taylor R. L.: Finite element method for solid and structural mechanics. Elsevier Butterworth Heineman , Sixth edition 2005.
[17] Aben H.: Integrated photoelasticity. Mc Graw-Hill Book Co., London, 1979.
[18] Laerman K. H.: The principle of integrated photoelasticity applied to experimental analysis of plates with nonlinear deformation. Proc. 7th Int. Conf. On Experimental Stress Analysis, Haifa, 1982.

Łączenie eksperymentu z analizą numeryczną w badaniach stanów zakrytycznych struktur cienkościennych

S t r e s z c z e n i e

W pracy przedstawiono metodykę umożliwiającą dokonywanie oceny modelu obliczeniowego oraz jego bieżących korekt, zapewniającą poprawną interpretację wyników nieliniowych analiz numerycznych ustrojów cienkościennych.

Proponowana metodyka opiera się na prowadzeniu, równolegle z nieliniową analizą numeryczną, badań doświadczalnych wybranych, newralgicznych elementów struktur nośnych. Zwrócono uwagę na uwarunkowania dotyczące przeprowadzania adekwatnego eksperymentu, wskazując na rolę badań modelowych, jako szybkiego i ekonomicznie uzasadnionego narzędzia badawczego możliwego do stosowania w trakcie projektowania cienkościennych ustrojów nośnych.

Przedstawione rozważania zilustrowano na przykładzie konstrukcji o stopniu złożoności geometrycznej i zakresach deformacji, charakterystycznych dla współczesnych rozwiązań stosowanych w ustrojach nośnych płatowców. Jako reprezentatywny przykład wybrano strefę struktury nośnej zawierającą obszerny wykrój, w której najwyższe poziomy i gradienty naprężeń pojawiają się w warunkach skręcania wywołującego stany deformacji zakrytycznej w zakresie obciążeń dopuszczalnych. Rozkłady naprężeń w tych zakresach deformacji stają się podstawą wyznaczania trwałości zmęczeniowej ustroju.